ALUMINA-CERIA-TZP NANOCOMPOSITES OBTAINED IN AN ALCOHOL MEDIUM BY TWO DIFFERENT PROCESSING ROUTES

L. Goyos, L.A. Díaz*, R. Torrecillas

Centro de Investigación en Nanomateriales y Nanotecnología (CINN), Consejo Superior de Investigaciones Científicas (CSIC) - Universidad de Oviedo (UO) - Principado de Asturias (PA), Parque Tecnológico de Asturias, 33428- Llanera (Asturias), Spain.
**la.diaz@cinn.es*

Keywords: nanocomposites, Al_2O_3-ZrO_2-CeO_2 ternary diagram system, biomaterials.

Abstract
Alumina-CeTZP nanocomposites have been obtained both, by applying a colloidal processing route in an alcohol medium, using alumina and alumina doped CeTZP nanopowders, and also by conventional powder mixtures of alumina and CeTZP with two different ceria contents (10 and 12 mol%). In all cases it has been possible to obtain fully dense nanocomposites after sintering under an air atmosphere. These nanocomposites, obtained using conventional processing techniques showed different sensibility to zirconia transformation, however, in all cases the mechanical properties were found to be very similar, showing flexural strength values in the range of 600–700 MPa and fracture toughness values of around 7-8 MPa $m^{-1/2}$. This paper compares the properties of these composites to those of conventional Y-TZP ceramics and discusses their suitability for different biomedical applications.

1 Introduction

Ceramic materials have been long considered as one of the best artificial substitutes for many types of prostheses, mainly hip, knee and dental implants [1][2]. Alumina was one of the first advanced ceramics to be used in orthopedic implants. However, due to its valuable properties, including higher toughness and improved fracture resistance, biomedical grade zirconia appeared as a good candidate to substitute alumina in biomedical applications. Up until 2005 more than 600,000 zirconia femoral heads were implanted worldwide, mainly in the USA and Europe [3, 4, 5]. The excellent mechanical behavior of zirconia is due to phase transformation toughening, which increases crack propagation resistance. The stress-induced phase transformation of zirconia involves the transformation of metastable tetragonal grains to the monoclinic phase at the crack tip, which, accompanied by volume expansion, induces compressive stresses [6, 7]. Given the moderate toughness of alumina and the issue related to the ageing of zirconia, there is a tendency to develop alumina-zirconia composites and/or nanocomposites. Some authors have developed zirconia doped alumina nanoceramics in order to improve the structural behavior of monolithic alumina. [8, 9]. De Aza et al. [10], and Affatato et al. [11] studied composites with different zirconia additions showing an important improvement of the mechanical properties without ageing. Some authors performed ageing studies on the alumina-zirconia system showing that 3Y-TZP-alumina composites containing over 16 vol% zirconia present significant ageing related to the percolation threshold, above

which a continuous path of zirconia grains allows transformation to proceed [12]. ZTA composite materials can be obtained by using different processing routes. Conventional methods include the mechanical mixing of powders using different milling systems, including attrition and ball milling. However, by following these routes it is not possible to achieve a fine microstructure free of agglomerates. To solve these processing limitations Schehl et al. [13] proposed a novel colloidal route through which they obtained a narrower distribution of zirconia grain sizes that could be tuned to be virtually identical or even smaller than the critical size corresponding to the spontaneous transformation of tetragonal phase zirconia to monoclinic phase zirconia. This route is based on controlling the heterogeneous precipitation of different precursors on the surface of ceramic and/or metallic particles and the subsequent crystallization of nanoparticles by subjecting the material to an adequate thermal treatment. By using this procedure [13] a major increase in fracture toughness (K_{IC}) compared to monolithic alumina can be achieved even when only a very small amount of zirconia phase (1,7 vol%) is present, reaching values of about 6.5 MPa.$m^{1/2}$. Another relevant achievement is the increase of the threshold stress intensity factor (K_{I0}), below which, no risk of slow crack growth propagation exists. In these nanocomposites K_{I0}/K_{IC} values are very close to one [14], something only known to happen in highly covalent materials. Other authors have proposed an improvement of the toughness of alumina composites by using ceria-stabilized zirconia (Ce-TZP) as the second phase. Ceria-doped tetragonal zirconia polycrystals (Ce-TZP) are known to have high toughness and high resistance to low-temperature thermal degradation, and, therefore, the addition of Ce-TZP to the alumina-zirconia nanocomposite is expected to increase its fracture toughness significantly. Thus, by controlling the content of ceria, the microstructure of the material and the percentage of transformed monoclinic zirconia [15], high values of fracture toughness (exceeding 16 MPa.$m^{1/2}$) can be achieved. Following this idea, some authors [16, 17, 18] have published a procedure for obtaining nanocomposites of alumina and Ce-TZP with an interpenetrated type nanostructure. The processing of these nanocomposites follows the traditional method of powder mixing; their mechanical properties and slow crack growth have been tested [19], obtaining K_{I0} values of approximately 4.5 MPa.$m^{1/2}$ and K_{IC} values of 8.8 MPa.$m^{1/2}$, which are both above the standards for biomedical prosthesis type monolithic alumina and zirconia. Moreover, new nanocomposites, in which nanometer-sized second phase particles are dispersed within a ceramic matrix and/or at grain boundaries, have shown significant improvements in strength and creep resistance, even at high temperatures, and assure an exciting future in different technological fields [20].

The present investigation reports the preparation and characterization of Ce-TZP/Al_2O_3 nanocomposites within the Al_2O_3-ZrO_2-CeO_2 system by following a simple colloidal processing route. Two different ceria contents were studied, 10 and 12 mol%. Moreover, a comparison between the colloidal method and the powder mixing route was made in terms of mechanical behaviour, phase transformation and ageing.

2 Materials and testing methods

The following materials were used: Ce-TZP (10 and 12 mol% CeO_2) from Daichi (Japan) with an average particle size of 35 nm (D_{50}) and a specific surface area of 15 m^2gr^{-1}; α-Al_2O_3 powder (TM DAR, Taimei Chemical Co.- Japan) with a specific surface area of 14,6 $m^2.gr^{-1}$ and an average particle size of 150 nm; aluminum chloride from Sigma-Aldrich (Spain); 99,97% absolute ethanol from Panreac (Spain) and 99,9% 2-Propanol from Panreac (Spain).

The procedure can be divided into two main steps:

1) Ce-TZP powders were coated with aluminum salt via precipitation. In order to do this, aluminum chloride ($AlCl_3$) was previously dissolved in absolute ethanol to form

different aluminium ethoxyde based products. The solution was subsequently added drop wise to a suspension of Ce-TZP powders in ethanol. The particle surface acts as the nucleating agent by stabilizing the deposited precursor; as a consequence, the selective deposition of an alumina amorphous layer takes place on the surface of the particles. After drying at 70ºC the powders were subjected to a thermal treatment at 950ºC to activate the formation of a γ-alumina (γA) transition phase.

2) Finally, the Ce-TZP coated powders were mixed with the alumina powders in a polypropylene container with the aid of zirconia balls durign 72 hours in order to guarantee the homogeneity of the mixture.

Three different compositions (all in vol%) were prepared in 2-Propanol:

1) γA coated Z10Ce + Al_2O_3 (A composition)
2) γA coated Z12Ce + Al_2O_3 (B composition)
3) Z10Ce + Al_2O_3 (C composition)

The chemical analyses of the three compositions are shown in Table 1. All materials have a final composition containing about 26 wt% of alumina.

	Al_2O_3	ZrO_2	CeO_2	SiO_2	Fe_2O_3	TiO_2	CaO	MgO	Na_2O	K_2O	P_2O_5	HfO_2	Ppc
A	26,20	63,91	8,12	<0,1	<0,03	<0,03	<0,06	<0,06	0,05	<0,03	<0,03	0,94	0,78
B	25,68	62,20	10,47	<0,1	<0,03	<0,03	<0,06	<0,06	<0,03	<0,03	<0,03	0,91	073
C	25,77	63,89	8,58	<0,1	<0,03	<0,03	<0,1	<0,03	<0,03	<0,03	<0,03	1,0	0,73

Table 1. Chemical analysis of compositions A, B and C. All values are given in wt %.

The Ce-TZP powders coated with amorphous alumina were thermally treated at different temperatures. Their phase evolution was studied using ^{27}Al MAS-NMR spectroscopy (Bruker MSL-400 spectrometer). ^{27}Al MAS-NMR spectra were recorded at 104,26 MHz with a 9,4 T external magnetic field. All measurements were carried out at room temperature and the samples were spun around an axis inclined 54º 44´ with respect to the magnetic field, at a spinning rate of 12 kHz (MAS technique). X-ray diffraction patterns were recorded in step scan mode (1 s/0,02º, 2θ) in the 2-65º (2θ) range by XDR D8 (Bruker, Germany) using CuKα radiation. Dynamic sintering tests were carried out in a dilatometer (Dil 802, Bähr, Germany) under air atmosphere at 1575ºC during 2h, with a heating rate of 10ºC/min. The density of the different samples was measured using the Archimedes method in deionized water. The temperature cycle applied was 1475ºC/1h for all compositions. Fracture toughness and bending strength measurements were carried out in an Instron 8562 testing machine by using a 4-point bending fixture with a bottom span of 35 mm and a top span of 10 mm. For the fracture toughness measurements (K_{Ic}) the single-edge-notched-beam (SENB) technique (a/w=0,4) was used. Beam specimens of dimensions 6×4×40 mm were used to measure fracture toughness (five test bars) and bending (ten test bars). The microstructure of the different nanocomposites was observed through a field emission scanning electron microscope (FE-SEM) (Zeiss Ultraplus, Germany) and through a transmission electron microscope (TEM) (JEOL-2000 EX-II, 200kV). The grain boundaries were observed both on polished and thermally attacked samples. The microhardness of the specimens, sintered at 1475ºC/1h, was determined using Vickers indentation technique (Buehler Micronet 5103 Model) by applying a load of 2,94 N. The reported microhardness values are the data averages obtained after thirty indentation tests. The volumetric fraction of the monoclinic phase was measured on as-sintered surfaces, as-sintered surfaces after 5h and 24h of ageing, polished surfaces and polished surfaces after a thermal treatment at 1200ºC for 15 minutes with and

without ageing for 5h and 24h. The volumetric fraction of the monoclinic phase was also measured on fractured surfaces following fracture toughness tests. The volumetric fraction of the monoclinic phase was measured from XRD patterns by using the expression proposed by Toraya et al. [21]:

$$V_m = \frac{1{,}311X_m}{1 + 0{,}311X_m}$$

Where X_m is the ratio of the peak intensity of the monoclinic phase, given by the equation:

$$X_m = \frac{I_m(\bar{1}11) + I_m(111)}{I_m(111) + I_m(\bar{1}11) + I_t(101)}$$

Where subscripts m and t represent the monoclinic and tetragonal phases, respectively.

Ageing test were performed on as-sintered and polished nanocomposite surfaces. They were carried out using a Tuttnauer Autoclave (2540EL) following the ISO 13356 2008 (E) norm, titled "Implants for surgery – Ceramic materials based on yttria-stabilized tetragonal zirconia (Y-TZP). The sintered probes were subjected to a steam atmosphere, a temperature of 134ºC, a pressure of 2 bars and holding times of 5 and 24 hours.

3 Results and discussion

The aluminum was detected to present an octahedral, tetrahedral and pentahedral coordination, typical of a γAl_2O_3 structure.

Table 2 shows the density obtained for the different materials after sintering at 1475ºC during 1h.

	A	**B**	**C**
Bulk density	2,65 gr/cm^3	2,61 g/cm^3	2,60 gr/cm^3

Table 2. Bulk density of compositions A, B and C after sintering at 1475ºC during 1h.

Figures 1A, 1B and 1C show the general microstructure of the studied compositions. As can be appreciated, the three microstructures are very similar; they are composed of a matrix of Ce-TZP grains, of size 400-500nm, and a homogeneously distributed second phase of alumina crystals, of an average size of 250nm.

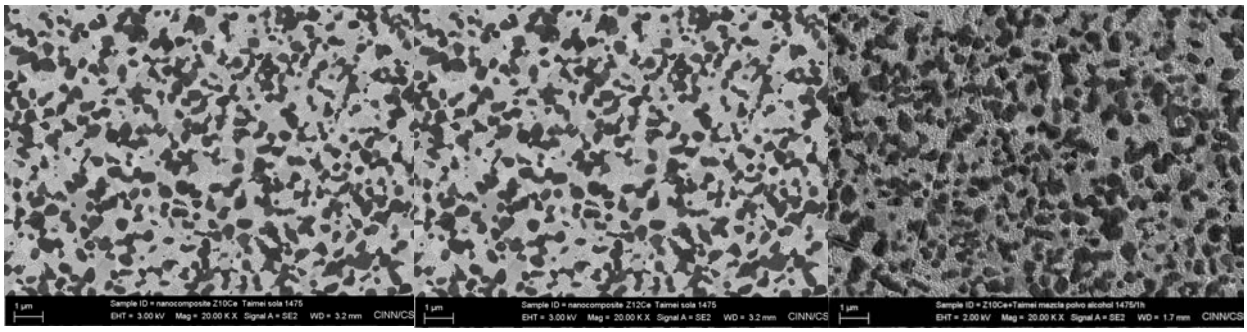

(1A) A composition **(1B)** B composition **(1C)** C composition

Figure 1. Microstructures of compositions A **(1A)**, B **(1B)** and C **(1C)**.

Table 3 shows the volumetric fractions of monoclinic phase zirconia (V_m) present on different surfaces of compositions A, B and C.

	Colloidal route		**Powder route**
	A ($V_{m\ total}$)	**B ($V_{m\ total}$)**	**C ($V_{m\ total}$)**
As-sintered	n.d.	n.d.	n.d.
As-sintered and ageing during 5h	n.d.	n.d.	n.d.
As-sintered and ageing during 24h	n.d.	n.d.	n.d.
Polished surfaces	15,73% ±3%	5,6%±3%	10,18% ±3%
Fractured surfaces	51,31% ±3%	12,4% ±3%	45,30% ±3%
Polished surfaces after thermal treatment 1200ºC/15min	n.d.	n.d.	n.d.
Polished surfaces after thermal treatment 1200ºC/15min and ageing during 5h	n.d.	n.d.	n.d.
Polished surfaces after thermal treatment 1200ºC/15min and ageing during 24h	n.d.	n.d.	n.d.

n.d. = not detected

Table 3. Volumetric fractions of monoclinic phase zirconia present on different surfaces of compositions A, B and C.

As can be seen in Table 3, the materials being studied do not present spontaneous phase transformation on their surface after sintering. Moreover, it can be appreciated that these materials do not undergo any hydrothermal ageing, not even after being subjected to very long and severe ageing treatments. However, both polishing and fracture processes do lead to the transformation, under tension, of part of the tetragonal zirconia to monoclinic zirconia. This effect is more pronounced for the materials containing 10 mol% ceria and, at the same time, it is more prominent in the case of the material obtained via the colloidal route, achieving in this last case almost 16 vol% of monoclinic phase zirconia against the 5,6 vol% obtained in the composition stabilized with 12 mol% ceria. This transformation process is reversible; in every case a posterior thermal treatment succeeds in transforming the totality of the monoclinic zirconia back to its initial tetragonal state. Furthermore, the surfaces subjected to this reversible process maintain their resistance to thermal ageing. This is important if we consider the possible relevance of these materials in CAD-CAM applications, as it allows the machining of both presintered and sintered materials which are subsequently subjected to thermal treatments in order to perform veneering with diverse types of enamel, in dental implantology, and any posterior transformation of zirconia to the monoclinic phase would lead to chipping, due to the volumetric changes associated to this transformation process. In this sense, these ceramic compositions present a major advantage with respect to the ytria stabilized zirconia materials that are currently being used for the fabrication of structures, abutments and implants.

It is interesting to compare the volumetric fractions of monoclinic zirconia found on the different fractured surfaces after performing the fracture toughness tests. It is possible to appreciate that the materials made of zirconia stabilized with 10 mol% ceria are much more transformable during the process of crack propagation and, for this reason, they could be expected to have a higher fracture toughness. Figure 2A shows the values of the flexural strength of compositions A, B and C. The values obtained are quite close to one another, although the nanocomposites containing zirconia stabilized with 10 mol% ceria show slightly higher values.

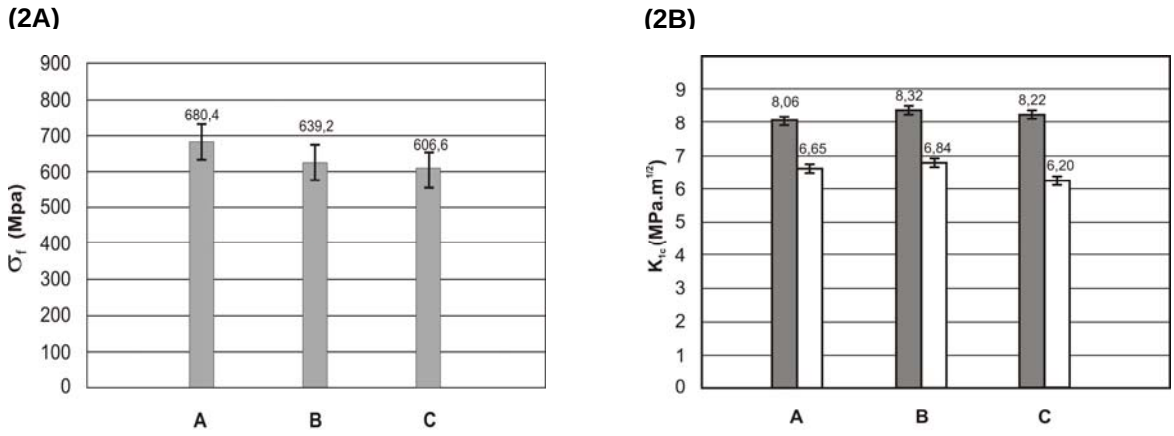

Figure 2. (2A) Flexural strength values of A, B and C. **(2B)** Fracture toughness values of A, B and C. The grey bars correspond to fracture toughness after saw cutting and the white bars correspond to fracture toughness after saw cutting and thermal treatment 1200°C/15min.

The values of fracture toughness obtained for these nanocomposites are very similar when using notched specimens (Figure 2B). Furthermore, it can be observed that the compression stresses that accumulate around the notch disappear when the specimens are subjected to thermal treatment (1200ºC/15min), decreasing the fracture toughness values in every case down to values between 6,2 and 6,6 MPa.m$^{1/2}$. The fact that a higher transformability does not imply higher mechanical property values is related to both intrinsic and extrinsic mechanisms, which are responsible for the resistance to crack propagation of these materials. Higher transformability implies higher plasticity, in the case of ceria stabilized zirconia. In fact, it is well known that Ce-TZP materials present high fracture toughness values but very low flexural strength values. In our case, the second phase, which consists of homogeneously distributed alumina within the matrix, sets the boundaries of the plastic deformation field, limiting both the deterioration of the flexural strength and the increase of the fracture toughness. Thus, it is important to find a compromise between the benefit of phase transformation and its associated plasticity, considered as positive reinforcement mechanisms, and the negative effect of their influence over the loss of rigidity, an effect that can be observed in metals with confronted fracture toughness and flexural strength values. It is now possible to design nanocomposite materials with different alumina contents in the second phase depending on the application for which the material is being designed. So, if we need components with complex shapes that will have to withstand stress concentrations, as is the case of a dental implant, it may be preferable to use a material with sufficient flexural strength and high fracture toughness. Figures 3A, 3B and 3C are SEM images of the fracture surfaces of composition A, B and C probes broken during fracture toughness tests.

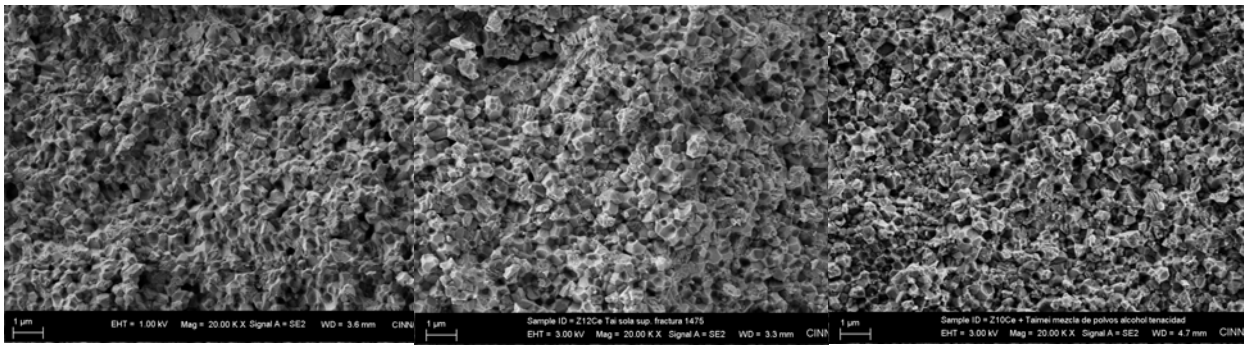

(3A) A composition **(3B)** B composition **(3C)** C composition

Figure 3. SEM images of the fracture surfaces of composition A **(3A)**, B **(3B)** and C **(3C)** probes broken during fracture toughness tests.

It is not possible to appreciate significant differences between Figures 3A, 3B and 3C. The fracture is intergranular in all cases and the transformation and plasticity suffered within the matrix can be observed in the form of multiple twins, associated with the process of phase transformation.

4 Conclusions

Ce-TZP/Al_2O_3 nanocomposites containing 10 and 12 mol% ceria show different fracture mechanisms, however, they present very similar flexural strength and fracture toughness values. The improvement that could be expected in the fracture toughness does not occur due to the coexistence of competing extrinsic and intrinsic mechanisms. In this case, the role of the rigid and homogeneously distributed second phase is crucial in order to limit the damage caused by the processes of phase transformation and plastic deformation. The stability of the mechanical properties is very important in the design of components for biomedical applications where complex shapes and functionalities require materials capable of maintaining their properties over time even if these are not exceptional. Materials such as zirconia Y-TZP show similar or worse mechanical properties because they are thermodynamically unstable, due to ageing phenomena. The equilibrium between the fracture toughness and the flexural strength of the nanocomposites mentioned above makes them optimal for multiple technological applications. Finally, it should be emphasized that by using conventional processing techniques, such as powder mixing, it is possible to attain very similar results to those achieved via colloidal processing routes where a better second phase distribution is obtained due to a more homogeneous dispersion of the particles in the liquid medium, in this case, alcohol.

5 References

[1] Hench, L.L. Bioceramics: From Concept to Clinic. *J. Am. Ceram. Soc.* **74**, pp. 1487-1510 (1991).

[2] Bayazit, V., Bayazit, M. and Bayazit, E. Evaluation of bioceramic materials in biology and medicine. *Digest Journal of Nanomaterials and Biostructures*, **7**, pp. 211-222 (2010).

[3] Chevalier, J. What future for zirconia as a biomaterial?. *Biomaterials*, **27**, pp. 535-543 (2006).

[4] Hench, L.L. Bioceramics. *J. Amer. Ceram. Soc.*, **81**, pp. 1705-1728 (1998).

[5] Piconi, C. and Maccauro, G. Zirconia as a ceramic biomaterial. *Biomaterials*, **20**, pp. 1-25 (1999).

[6] Garvie, R.C., Hannink, R.H.J., Pascoe, R.T. Ceramic Steel?. *Nature*, **258**, pp. 703-704 (1975).

[7] Green, D.J., Hannink, R.H.J., Swain, M.W. Transformation toughening of ceramics. *Boca Raton, FL: CRS Pres, Inc.*, pp. 232 (1989).

[8] Claussen N. Fracture Toughness of Al_2O_3 with an Unstabilized ZrO_2 Dispersed Phase. *J. Am. Ceram. Soc.*, **59** (1-2), pp. 49-51 (1976).

[9] Lange, F.F., Transformation toughening: Part 4 Fabrication, fracture toughness and strength of Al2O3-ZrO2 composites. *J. Mater. Sci.,* **17**, 247-254 (1982).

[10] De Aza, A.H., Chevalier, J., Fantozzi, G., Schehl, M. and Torrecillas, R. Crack growth resistance of alumina, zirconia and zirconia toughened alumina ceramic for joint prostheses. *Biomaterials*, **23**, pp. 937-945 (2002).

[11] Affatato, S.,Testoni, M., Cacciari, G.L., Toni, A. Mixed oxides prosthetic ceramic ball heads. Part 2: effect of the ZrO_2 fraction on the wear of ceramic joints. *Biomaterials*, **20**, pp. 1925-1929 (1999).

[12] Pecharromán, C., Bartolomé, J.F., Requena, J., Moya, J.S., Deville, S., Chevalier, J., Fantozzi, G., and Torrecillas, R. Percolative Mechanism of Aging in Zirconia-Containing Ceramics for Medical Applications. *Advanced Materials*, **15**, pp. 507-511 (2003).

[13] Schehl, M., Díaz, L.A., and Torrecillas, R. Alumina nanocomposites from powder-alkoxide mixtures. *Acta Mater*, **50** (5), pp.1125-1139 (2002).

[14] Chevalier, J., Deville, S., Fantozzi, G., Bartolomé, J.F., Pecharromán, C., Moya, J.S., Diaz, L.A. and Torrecillas, R. Nanostructured ceramic oxides with a slow crack growth resistance close to covalent materials. *Nano Letters*, **5**, pp. 1297-1301 (2005).

[15] Tsukuma, K. Mechanical properties and thermal stability of CeO_2 containing tetragonal zirconia polycrystals. *Am. Ceram. Soc. Bull.*, **65**, 1386-1389 (1986).

[16] Nawa, M., Yamaguchi, K., Toki, M., U.S. Patent 7012036 of March 14, (2006).

[17] Nawa, M. Nakamoto, S. Sekino, T. and Niihara, K. Tough and Strong Ce-TZP/Alumina Nanocomposites Doped with Titania. *Ceramics International*,; **24**, pp.497-506 (1998).

[18] Nawa M. and Niihara K., Ceramic based nanocomposites. In: "Metal and Ceramic Matrix Composites", Edited by B. Cantor, F. Dunne and I. Stone, IOP Publishing Ltd., chapter 22, (2004).

[19] Benzaid, R., Chevalier, J., Saâdaoui M, Fantozzi G, Nawa M, Diaz, L.A., Torrecillas, R., Fracture toughness, strength and slow crack growth in a ceria stabilized zirconia–alumina nanocompositefor medical applications. *Biomaterials,* **29** (27), pp 3636–3641 (2008).

[20] Torrecillas, R., Moya, J. S., Díaz, L.A., Bartolomé, J.F., Fernández, A., López-Esteban, S. Nanotechnology in joint replacement, Wiley Interdiscip Rev Nanomed Nanobiotechnol. *Wiley Interdiscip. Rev. Nanomed. Nanobiotechnol.* **1** (5), pp. 540-552 (2009).

[21] Toraya, H., Yoshimura, M., Somiya, M. Calibration curve for quantitative analysis of the monoclinic tetragonal Zr=2 system by X-rays diffraction. *J. Am. Ceram. Soc.*, **67**, pp. 119-121 (1984).